Journal of Comparative Physiology B
https://doi.org/10.1007/s00360-023-01487-4

ORIGINAL PAPER

Investigating nitrogen movement in North Pacific spiny dogfish (*Squalus acanthias suckleyi*), with focus on UT, Rhp2, and Rhbg mRNA abundance

J. Lisa Hoogenboom[1,2] · **W. Gary Anderson**[1,2]

Received: 17 August 2022 / Revised: 15 March 2023 / Accepted: 14 April 2023

Abstract
For ureosmotic marine elasmobranchs, the acquisition and retention of nitrogen is critical for the synthesis of urea. To better understand whole-body nitrogen homeostasis, we investigated mechanisms of nitrogen trafficking in North Pacific spiny dogfish (*Squalus acanthias suckleyi*). We hypothesized that the presence of nitrogen within the spiral valve lumen would affect both the transport of nitrogen and the mRNA abundance of a urea transporter (UT) and two ammonia transport proteins (Rhp2, Rhbg) within the intestinal epithelium. The in vitro preincubation of intestinal tissues in NH_4Cl, intended to simulate dietary nitrogen availability, showed that increased ammonia concentrations did not significantly stimulate the net uptake of total urea or total methylamine. We also examined the mRNA abundance of UT, Rhp2, and Rhbg in the gills, kidney, liver, and spiral valve of fasted, fed, excess urea fed, and antibiotic-treated dogfish. After fasting, hepatic UT mRNA abundance was significantly lower, and Rhp2 mRNA in the gills was significantly higher than the other treatments. Feeding significantly increased Rhp2 mRNA levels in the kidney and mid spiral valve region. Both excess urea and antibiotics significantly reduced Rhbg mRNA levels along all three spiral valve regions. The antibiotic treatment also significantly diminished UT mRNA abundance levels in the anterior and mid spiral valve, and Rhbg mRNA levels in the kidney. In our study, no single treatment had significantly greater influence on the overall transcript abundance of the three transport proteins compared to another treatment, demonstrating the dynamic nature of nitrogen balance in these ancient fish.

Keywords Transporter · Urea · Ammonia · Methylamine · UT · Rhp2 · Rhbg · Elasmobranch

Introduction

Urea is a critical component in the osmoregulatory strategy of marine elasmobranchs (Smith 1929, 1936), but the nitrogen required for its synthesis can be limited due to their putative intermittent feeding behaviors, and the need for nitrogen for obligatory somatic processes (Wood 2001; Bucking 2015). Urea is also energetically expensive to produce (Anand and Anand 1993; Walsh and Mommsen 2001); therefore, to reduce energetic costs and maintain internal nitrogen homeostasis, these animals must possess physiological mechanisms capable of retaining urea. Transport proteins capable of moving nitrogenous compounds, such as urea and ammonia, across tissues are one such mechanism. The first urea transporter (UT) identified in a marine fish was shark UT (ShUT) (Smith and Wright 1999). The mRNA of ShUT was demonstrated in the kidney and brain of the spiny dogfish (*Squalus acanthias suckleyi*), with related mRNA sequences found in the gills, liver, muscle, rectal gland, red blood cells, and spiral valve (Smith and Wright 1999). ShUT was identified as a facilitative transporter that shared 66% identity to the rat UT-A2 transport protein, and when expressed in *Xenopus* oocytes, it induced a tenfold increase in ^{14}C-urea uptake that could be inhibited by the general transport blocker phloretin (Smith and Wright 1999).

Subsequently, UT-A-like urea transporters (LeMoine and Walsh 2015) have been found in many tissues (e.g., brain, gills, heart, liver, muscle, rectal gland, red blood cells, renal tissue, spiral valve, and testes) of several marine

Communicated by B. Pelster.

✉ J. Lisa Hoogenboom
lisa.hoogenboom@umanitoba.ca

[1] Department of Biological Sciences, University of Manitoba, Winnipeg, MB R3T 2N2, Canada

[2] Bamfield Marine Sciences Centre, 100 Pachena Road, Bamfield, BC V0R 1B0, Canada

Published online: 10 May 2023

elasmobranchs, including the Japanese banded houndshark (*Triakis scyllium*) (Hyodo et al. 2004), the Atlantic stingray (*Dasyatis sabina*), the winter skate (*Leucoraja ocellata*) (Janech et al. 2003, 2006, 2008), and the little skate (*Leucoraja erinacea*) (Morgan et al. 2003). Immunohistochemical studies using the banded houndshark showed the renal UT to be exclusively expressed in the collecting tubules, indicating that it is likely responsible for the reabsorption of urea from the primary urine (Hyodo et al. 2004; Yamaguchi et al. 2009). The reabsorption and retention of filtered urea (Hyodo et al. 2014) would act as an important component of nitrogen homeostasis in these animals, acting to conserve valuable nitrogen from urinary excretion.

Smith and Wright (1999) first identified a UT transcript in the intestinal tissue of the spiny dogfish, and the mRNA abundance of UTs along the length of the spiral valve in the little skate was reported by Anderson et al. (2010). The UT in the little skate showed an increasing trend in transcript abundance from the anterior to the posterior region of the spiral valve, and the overall abundance was orders of magnitude lower than the renal tissue (Anderson et al. 2010). As the main site of urea uptake (Liew et al. 2013), as well as a probable contributor to the synthesis of urea via the ornithine-urea (OUC) (Kajimura et al. 2006), UTs within the intestinal tissues could facilitate the trafficking of urea between the lumen of the gut and plasma.

Due to their ureosmotic nature, previous studies investigating nitrogen transport and utilization in marine elasmobranchs have focused on urea and the organs involved in its synthesis, retention, and loss. More recently, attention has turned to the acquisition and transport of ammonia, especially along the spiral valve (Anderson et al. 2010; Wood et al. 2019; Hoogenboom et al. 2020; Weinrauch et al. 2020). The use of urea as an osmolyte necessitates the retention of ammonia and its conversion to glutamine, the nitrogen-donating substrate for the marine elasmobranch OUC (Anderson and Casey 1984; Anderson 1991). Therefore, the acquisition, retention, and transport of ammonia is of considerable interest, and further investigations may lead to a better understanding of whole-body nitrogen homeostasis within these animals.

Research into the transport of ammonia has expanded considerably since the discovery that Rhesus-like (Rh) glycoprotein transporters have the capacity to transport ammonium (Marini et al. 1997, 2000; Westhoff et al. 2002). The first identification of a Rh transporter in an elasmobranch was Rhbg in the spiral valve, kidney, and rectal gland of the little skate (Anderson et al. 2010). Subsequently, the mRNA of Rhbg has also been demonstrated in the brain, gills, kidney, liver, muscle, rectal gland, spiral valve, and cardiac and pyloric stomachs of *S. a. suckleyi* (Nawata et al. 2015a, b). Within the spiral valve of the little skate, Rhbg mRNA abundance was orders of magnitude higher than the UT, and showed a trend of increasing abundance from the anterior to the posterior region (Anderson et al. 2010). Another ammonia transporter, Rhp2, was first identified in the renal collecting tubules of the banded houndshark kidney (Nakada et al. 2010). Rhp2 mRNA has since been demonstrated in the red blood cells, brain, gills, spiral valve, kidney, liver, muscle, rectal gland, and cardiac and pyloric stomachs of *S. a. suckleyi* (Nawata et al. 2015a). The presence of ammonia transporters in these ureosmotic animals highlights the importance of regulated ammonia trafficking across various tissues.

In addition to the mechanisms necessary to transport and regulate the movement of urea and ammonia, another aspect of nitrogen homeostasis that is gaining research attention is the role of the gastrointestinal (GI) microbiome in nitrogen homeostasis. The presence of urease, a microbial enzyme, was demonstrated within the GI tract of *S. a. suckleyi* (Wood et al. 2019). Urea is a metabolic dead-end for most vertebrates, and the presence of a microbial enzyme capable of catabolizing urea into ammonia may provide a route for nitrogen recycling (Mobley and Hausinger 1989; Stewart and Smith 2005). In vitro flux studies with *S. a. suckleyi* demonstrated a net efflux of urea across the intestinal tissues of fasted animals (Liew et al. 2013; Anderson et al. 2015). It was proposed that the urea efflux into the intestinal lumen may be recycled by GI microbial urease to liberate nitrogen for use by the microbiome or the host (Wood et al. 2019), similar to the urea-nitrogen salvaging (UNS) in ruminants (Stewart and Smith 2005).

To better understand the in vitro urea flux and ammonia accumulation that occurs along the dogfish spiral valve, the goal of this study was to examine mechanisms potentially responsible for nitrogen trafficking. We examined the flux of nitrogen across intestinal tissues mounted in Ussing chambers using radiolabelled urea and the ammonia analog, methylamine as a proxy for the movement of ammonia. We hypothesized that nitrogen availability, simulated by the preincubation of the spiral valve tissues in NH_4Cl, would affect the movement of the radiolabelled substrates from the mucosal medium to the serosal. We predicted increased nitrogen availability would increase the uptake of urea and methylamine, as a method of nitrogen acquisition and retention. We also examined the mRNA abundance of three nitrogen transport proteins (UT, Rhp2, Rhbg) in fasted and fed dogfish to understand how nitrogen availability may affect urea and/or ammonia trafficking. Additionally, as increased urea in the diet (Hoogenboom et al. 2020), or an antibiotic treatment intended to diminish the GI microbiome (MacPherson et al. 2022) may influence ammonia accumulation in the intestine of the dogfish, we examined the transcript abundance levels of the three transport proteins in dogfish fed 700 mM urea or treated with antibiotics via gavage. In addition to investigating the movement of nitrogen

across the spiral valve (site of nitrogen acquisition), we also examined the mRNA abundance of the nitrogen transporters in the gills and kidney (nitrogen loss and retention) and liver (urea synthesis). We hypothesized that prandial nitrogen would affect the mRNA abundance of the transport proteins. We predicted that the level of transcript abundance would be dependent on the preservation or loss of nitrogen necessary for the animals to maintain whole-body nitrogen homeostasis.

Methods

Animals

Male North Pacific spiny dogfish (*S. a. suckleyi*) were collected by rod-and-reel in Barkley Sound, British Columbia in July and August, 2017–2019 (2.12 ± 0.05 kg). Animals were held at Bamfield Marine Sciences Centre in 1,500 L outdoor covered flow-through circular tanks. Sea water was held at a constant temperature (12 ± 1.0 °C) and salinity (30 ± 2.0 ppt) with a natural photoperiod. All protocols were approved by the Animal Care Committee at Bamfield Marine Sciences Centre (RS-17-03, RS-18-03, and RS-19-03) within the guidelines of the Canadian Council on Animal Care and appropriate collection permits for scientific research as issued by Fisheries and Oceans, Canada (XR 135 2017, XR 149 2018, and XR 99 2019).

Feeding

All dogfish were fasted for 7 days to ensure complete digestion and evacuation of their GI tracts, and ensure that all animals were in a similar metabolic state with similar internal resource demands (Jones and Geen 1977; Kajimura et al. 2006; Wood et al. 2007a). For the fed animals, following light anesthesia (tricaine methanesulfonate, MS-222; 100 ppm. Syndel Labs, Vancouver, BC, Canada), dogfish were weighed and force-fed via gavage according to previously published methods (Hoogenboom et al. 2020). Frozen Atlantic herring (*Clupea harengus*; Rhys Davis, Sidney B.C.) were thawed and blended into a slurry with minimal filtered seawater (no more than 5% seawater by mass). For the excess urea dogfish, urea (Sigma-Aldrich) was added to the herring-slurry to a final concentration of 700 mM (Hoogenboom et al. 2020), and fed via gavage directly into the cardiac stomach. We chose a concentration beyond that normally found within the tissues and plasma of *S. a. suckleyi* in an effort to examine the nitrogen handling capabilities of these animals, as well as to not mask the potential results of the exogenous urea uptake by the endogenous concentrations found within the animal. The antibiotic (AB) treated dogfish received six treatments of antibiotic cocktail (in mg kg^{-1} body mass: 75 ampicillin, 75 chloramphenicol, 20 sisomicin, and 20 penicillin) made with ammonia-free elasmobranch Ringer's (in mM: 400 urea, 257 NaCl, 80 TMAO, 7 Na_2SO_4, 6 $NaHCO_3$, 5 glucose, 4 KCl, 3 $MgSO_4$, 2 $CaCl_2$, 0.1 $NaHPO_4$; pH 7.8). Every 24 h, the dogfish were lightly anesthetized (MS-222; 100 ppm), and received the antibiotic cocktail via gavage directly into the cardiac stomach. On day 6, during the final anesthesia and antibiotic cocktail administration, the dogfish were fed the herring-slurry with $^{15}NH_4Cl$ to a final concentration of 7 mM (MacPherson et al. 2022). The use of ^{15}N was necessary for an additional study (Hoogenboom and Anderson, in revision) and we assume that the ^{15}N labeled nitrogen behaves in the same way as the abundant ^{14}N. The fed and excess urea dogfish digested for 20 h, and the AB-treated dogfish digested for 72 h prior to immersion in a terminal dose of anesthetic (MS-222; 250 ppm), and collection of tissues for in vitro flux and molecular studies.

Tissue collection

For the mRNA abundance of the transport proteins, the following tissues were collected: anterior, mid, and posterior intestinal folds from the spiral valve, the gills, kidney, and liver. It should be noted that gill and kidney samples were not collected from the excess urea treatment group. When a longitudinal incision is made along the length of the spiral valve of *S. a. suckleyi*, the internal structure consists of 14–15 folds that slow the passage of food and increase the surface area for nutrient absorption (Chatchavalvanich et al. 2006; Bucking 2015; Leigh et al. 2021). We classified the anterior region of the spiral valve as the first 4−5 folds, the mid region as the middle 4−5 folds, and the posterior region as the remaining 4–5 folds before the colon (Anderson et al. 2010). All tissues were rinsed in ammonia-free elasmobranch Ringer's to remove any chyme or residual blood, placed into RNAlater (Invitrogen; ThermoFisher), and left at room temperature for 24 h prior to storage at − 80 °C until analysis. For the spiral valve folds, only the epithelial layer was used for mRNA abundance quantification; the epithelium was carefully scraped from the underlying connective/muscle layer using a No. 10 scalpel blade (Anderson et al. 2010).

Ussing chamber flux studies

To examine the movement of urea and methylamine (MA) across the spiral valve, folds from the three regions were mounted in Ussing chambers. Seven day fasted dogfish were used to examine bidirectional flux in the absence of digestive processes. To simulate the serosal (i.e., basolateral) side of the tissues, the mucosal epithelial layer was carefully scraped from one side of the fold (now nominally referred

to as the serosal side) using a No. 10 scalpel blade, while leaving the epithelium intact on the other side (the mucosal side), as per previously published protocols (Anderson et al. 2015). Removal of the epithelial layer from one side of the fold limited the role of epithelium transport for the substrates of interest. For consistency, the epithelial layer was always removed from the distal side of the fold, which points toward the colon of an intact spiral valve.

For paired bidirectional flux experiments, the one-side-scraped intestinal folds were cut in half, mounted on two separate tissue holders with a 0.3 cm^2 aperture (P2310; Physiologic Instruments), and placed into the Ussing chamber (EM-CSYS-2; Physiologic Instruments) with 5 mL ammonia-free elasmobranch Ringer's added to each side (as above). The chambers were supplied with specialty gas mix (99.5% O_2: 0.5% CO_2) and cooled to 12 ± 1 °C with a recirculating chiller. To determine influx, a radiolabelled substrate, either ^{14}C-urea (0.125 μCi mL^{-1}; PerkinElmer, USA) or ^{14}C-methylamine hydrochloride (MA), a proxy for ammonia (0.05 μCi mL^{-1}; Moravek Biochemicals, CA, USA) was added to the mucosal side of the chamber. To determine efflux in the matched paired chamber, the radiolabelled substrate was added to the serosal side. Immediately following the addition of the radiolabelled substrate, a sample (0.02 mL) was collected to represent time zero, and again following a 3 h incubation period. The 0.02 mL samples were added to 1 mL deionized water and 4 mL scintillation cocktail (Ultima Gold, PerkinElmer), and the radioactivity was counted using a liquid scintillation counter (Beckman LS6000, Beckman Coulter, CA, USA). Sampling of the incubation fluid from both sides of the chamber following the addition of the labelled substrate also allowed us to ensure that preparation of the spiral valve folds did not result in holes and unregulated leakage of the radiolabelled substrate across the tissue. The presence of holes would have been evidenced by a rapid equilibrium of the radiolabel between the two chambers, which did not occur in any of our experiments. The linearity of the flux rates was not examined in this study, as previous research from our lab has demonstrated linear flux rates for radiolabelled urea across the spiral valve folds of spiny dogfish, as well as demonstrating the viability of the tissues over the incubation period (Anderson et al. 2015).

The influx (Jms) of ^{14}C-urea or ^{14}C-MA was determined by the appearance of the radiolabelled substrate on the serosal side of the preparation, as determined by an increase in radioactivity after 3 h compared to time zero, and was calculated as follows:

$$\text{Jms} = \frac{V \times (R2 - R1)}{(R3 \div \text{M}) \times \text{SA} \times T},$$

where Jms (urea, μmol cm^{-2} h^{-1}; MA, *f*mol cm^{-2} h^{-1}) is the movement of the radiolabelled substrate from the mucosal to the serosal side; *V* (mL) is the volume of elasmobranch Ringer's on the serosal side of the chamber (4.98 mL); *R*2 and *R*1 are the radioactivates (cpm mL^{-1}) on the serosal side of the chamber taken at the end and beginning of the incubation, respectively, as measured by the liquid scintillation counter; R3 is the radioactivity (cpm mL^{-1}) on the mucosal side of the chamber at time zero, as measured by the liquid scintillation counter; M is the moles of substrate present in the elasmobranch Ringer's (urea: 400 μmol mL^{-1}; MA: 2.8 pmol mL^{-1}); SA is the surface area of the tissue holder aperture (0.03 cm^{-2}); and *T* is the incubation time of the radiolabelled substrate (3 h).

The efflux (Jsm) of the radiolabelled substrates was determined by the appearance of the substrate on the mucosal side of the intestinal preparation 3 h after the start of the experiment, and calculated as above, except Jsm (μmol cm^{-2} h^{-1}; *f*mol cm^{-2} h^{-1}) is the movement of the radiolabelled substrate from the serosal to the mucosal side; *V* is the volume on the mucosal side of the chamber; *R*2 and *R*1 are the radioactivates of the mucosal side, and *R*3 is the radioactivity on the serosal side at time zero.

The net flux (μmol cm^{-2} h^{-1}; *f*mol cm^{-2} h^{-1}) of the radiolabelled substrates was calculated as follows:

$$\text{Jnet} = \text{Jms} - \text{Jsm},$$

where a positive Jnet value indicates a net influx of substrate from the mucosal to serosal side of the preparation, while a negative value indicates a net efflux from serosal to mucosal.

To examine if nitrogen availability, resulting from the catabolism of dietary amino acids into ammonia affects the uptake of lumenal urea and MA, the intestinal tissues were preincubated in NH_4Cl (0–10 mM; Sigma-Aldrich) added to the Ringer's on the mucosal side of the Ussing chamber for 2 h. To ensure that the movement of urea or MA was not influenced by the NH_4Cl concentration gradient, following the 2 h preincubation, the Ringer's containing the NH_4Cl was removed from both sides of the preparation and flushed 3× with fresh Ringer's. 5 mL of fresh ammonia-free Ringer's was again added to both sides of the preparation, along with either ^{14}C-urea or ^{14}C-MA, as described above, for a paired 3 h bidirectional flux experiment.

mRNA abundance of transport proteins

Total RNA was isolated as previously described (Anderson et al. 2010) under RNase-free conditions. The scraped epithelial layer from the spiral valve folds, or the whole tissues from the gills, kidney, or liver were homogenized (TissueLyser II; Qiagen) in TRIZOL reagent (Invitrogen). Following chloroform, isopropanol, and ethanol precipitation,

RNA was stored in RNA storage solution (Ambion; Thermofisher), and RNA concentrations and were determined using Nanodrop (2000 Spectrophotometer; Thermofisher), and tested for purity by polymerase chain reaction (PCR; 40 cycles) using 1 µg Dnase-treated RNA (DNase1; Thermofisher). RNA samples (1 µg) showing no PCR-product (DNA free) were reverse transcribed into cDNA using iScript RT Supermix (Bio-Rad). PCR products were run on a 1.5% agarose electrophoresis gel (100 mA/100 V, 40 min) with TAE buffer (Tris base, acetic acid, EDTA) and ethidium bromide, and visualized under UV light.

Primers for the nitrogen transporters (UT, Rhp2, Rhbg) were designed based on published sequences for *S. a. suckleyi* (Table 1) (Nawata et al. 2015a, b), verified by sequencing through the TCAG DNA Sequencing Facility (The Hospital for Sick Children, Toronto, Canada) and using GenBank BLAST Sequence Analysis Tool (National Centre of Biotechnology Information). The mRNA abundance of the transport proteins was quantified using reverse transcription quantitative real-time PCR (RT-qPCR). Standard curves for primer efficiency were generated using a serial dilution series beginning with 1 µL cDNA. A minimum R^2 value of 0.98 was required, with an efficiency between 99 and 103%. RT-qPCR (CFX Connect; Bio-Rad) was performed using 50 ng cDNA, 4 µM of both the forward and reverse primer, and SSOAdvanced Universal SYBR Green Supermix (Bio-Rad) in a 10 µL reaction. RT-qPCR products were verified by melt curve analysis and visualization of product size via electrophoresis and ethidium bromide/UV. For relative mRNA abundance of transporters, β-actin (ACTB1) was used as an internal standard. Suitability of ACTB1 was evaluated by RT-qPCR and showed similar abundance levels across tissues and treatments (data not shown). All RT-qPCR data were converted to delta delta Ct values, and a modified $2^{-\Delta\Delta Ct}$ method was used, which calculated the efficiencies of the individual primers rather than assuming 100% efficiency (Rao et al. 2013).

Statistical analysis

Data are presented as mean ± sem within the text and figures. Statistical analyses were conducted using *RStudio* (R Core Team 2017) and figures were produced using the *ggplot2* package (Wickham 2009). For multiple comparisons, one-way analysis of variance (ANOVA) was performed for the urea and MA net flux Ussing chamber data (Figs. 1B, 2B, 3b, 4b) and data were checked for normality (Shapiro–Wilk) and homogeneity of variance (Levene's test). Two-way ANOVA was performed for the urea and MA influx/efflux Ussing chamber data (Figs. 1A, 2A, 3A, 4A), as well as the mRNA abundance of the transport proteins (Figs. 5, 6). Tukey's post hoc test was used to detect significant differences, which were significant when $p < 0.05$. Data were checked for normality (Shapiro–Wilk) and homogeneity of variance (Levene's test); however, where the data analyzed by two-way ANOVA departed from one or both of the assumptions required for

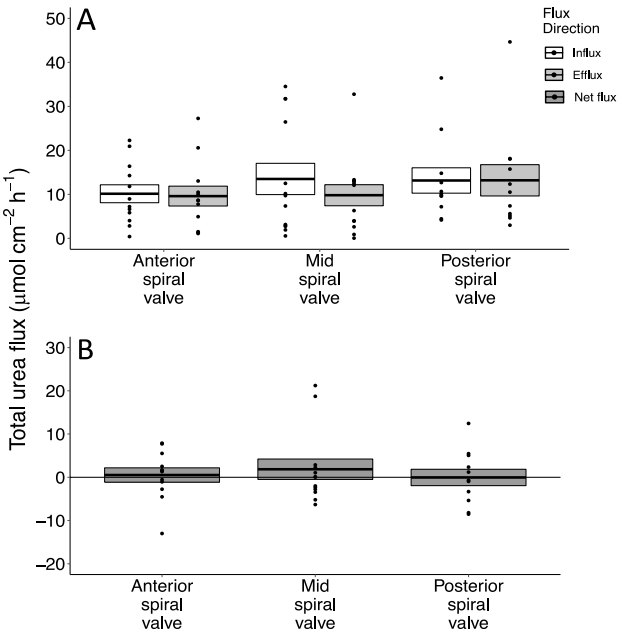

Fig. 1 Total urea flux across intestinal spiral valve folds from 7 day fasted North Pacific spiny dogfish (*Squalus acanthias suckleyi*). Tissues mounted in Ussing chambers and incubated for 3 h. **A** influx and efflux; two-way ANOVA, $p < 0.05$. **B** net flux; one-way ANOVA, $p < 0.05$. Horizontal line within the boxplots indicates mean, and the upper and lower box boundaries indicate sem, with individual data points represented as black dots ($n = 12$)

Table 1 Primers used in reverse transcription quantitative real-time PCR (RT-qPCR) targeting a urea transporter (UT), two Rhesus glycoprotein ammonia transporters (Rhp2, Rhbg), and β-actin (ACTB1) in *Squalus acanthias suckleyi*

Gene	Forward primer 5′–3′	Reverse primer 5′–3′	Product size (bp)	Accession no	Efficiency (%)	T_m melting temperature (°C)
UT	ACTGAGATCAGGCCATGTA	GCTGCAACAGGACACTAC	90	AF257331	101	60
Rhp2	GGAGCTGCTGAAGATCAAGG	AGACCCACAGCAACAAGGTC	182	KJ960198	99	56
Rhbg	TTCGAGTCCGCGGTCTT	CCCGAAGGTGTGGATGGT	96	KJ960197	103	60
ACTB1	TGCACTGGACTTTGAACAGG	TTCCACAGGATTCCATACCC	164	AY581300	99	56

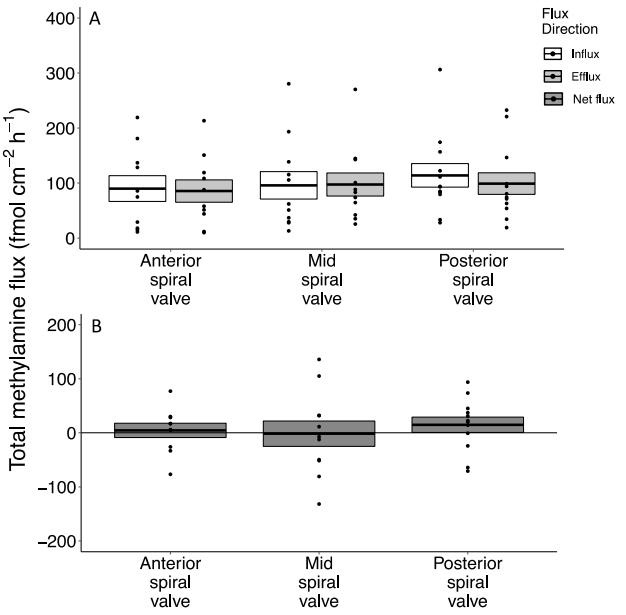

Fig. 2 Total methylamine (MA) flux across intestinal spiral valve folds from 7 day fasted North Pacific spiny dogfish (*Squalus acanthias suckleyi*). Tissues mounted in Ussing chambers and incubated for 3 h. **A** Influx and efflux; two-way ANOVA, $p < 0.05$. **B** Net flux; one-way ANOVA, $p < 0.05$. Horizontal line within the boxplots indicates mean, and the upper and lower box boundaries indicate sem, with individual data points represented as black dots ($n = 11$)

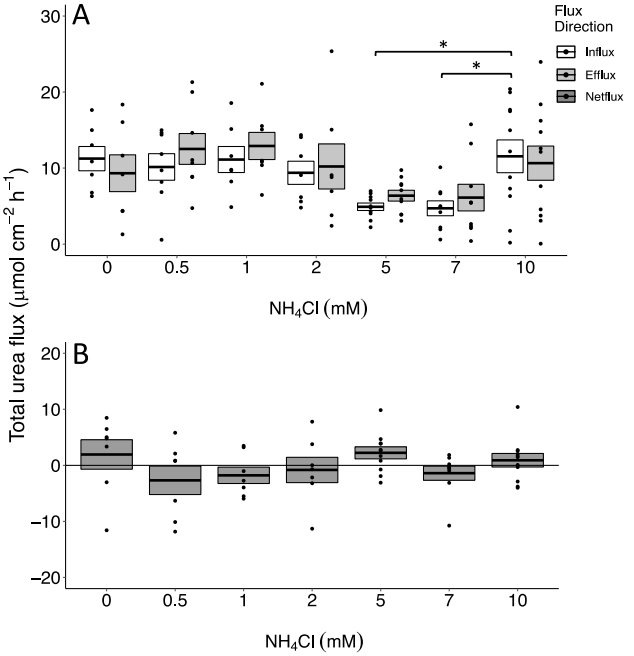

Fig. 3 Total urea flux across intestinal spiral valve folds from 7 day fasted North Pacific spiny dogfish (*Squalus acanthias suckleyi*). Tissues mounted in Ussing chambers and preincubated with NH_4Cl (0–10 mM) for 2 h before preincubation solution was removed, tissues rinsed with fresh Ringer's, and ^{14}C-urea added for 3 h incubation. **A** Influx and efflux; two-way ANOVA, $p < 0.05$. **B** Net flux; one-way ANOVA, $p < 0.05$. * Denotes significant difference. Horizontal line within the boxplots indicates mean, and the upper and lower box boundaries indicate sem, with individual data points represented as black dots ($n = 7$–11)

parametric analysis, and transformation of the data did not result in normality or homogeneity of variance, analyses of the non-normal data were performed via the above described parametric tests without transforming the data. This was due to the lack of comparable non-parametric analyses equivalent to the two-way ANOVA sufficient to evaluate our data containing two categorical variables, as well as the robust nature of the ANOVA test that allows it to function reliably even when parametric assumptions are violated (Zar 1984). Where a range in sample size (n) is indicated in the figure caption, variation is due to animal availability; no data were removed as statistical outliers. For paired Ussing chamber flux experiments, sample size was the same for both influx and efflux, allowing for net flux calculations.

Results

Bidirectional flux studies

The direction of total urea flux (influx or efflux) was examined across the three spiral valve regions (anterior, mid, and posterior). There was no interaction between region and direction ($F_{2,66} = 0.006$, $p = 0.99$), and no significant difference in the direction of total urea flux across the three regions ($p > 0.6$), or within the regions ($p > 0.4$) (Fig. 1A). All spiral valve regions showed no net flux of total urea ($p > 0.7$) (Fig. 1B). For total MA flux, there was no significant interaction between region and direction ($F_{2,60} = 0.08$, $p = 0.9$), and no significant differences in total MA influx or efflux between the three regions ($p > 0.7$), or within the regions ($p > 0.6$) (Fig. 2A). All spiral valve regions showed no net flux of total MA ($p > 0.7$) (Fig. 2B).

To simulate dietary nitrogen availability, and examine if the transport of total urea or total MA was dependent upon a threshold of ammonia (i.e., nitrogen) availability within the spiral valve lumen, tissues from 7 day fasted *S. a. suckleyi* were mounted in Ussing chambers with NH_4Cl (0–10 mM) added to the mucosal (i.e., lumenal) side. For total urea, there was no significant interaction between concentration and direction ($F_{6,104} = 0.35$, $p > 0.9$), and no significant differences between influx and efflux at any NH_4Cl preincubation concentration ($p > 0.1$), except a significant decrease in the influx of total urea at 5 and 7 mM NH_4Cl compared to 10 mM ($p < 0.02$) (Fig. 3A). All preincubation concentrations showed no net flux of total urea ($p > 0.9$), and no significant differences across the NH_4Cl preincubation concentrations ($p > 0.3$) (Fig. 3B). For total MA, there was no significant

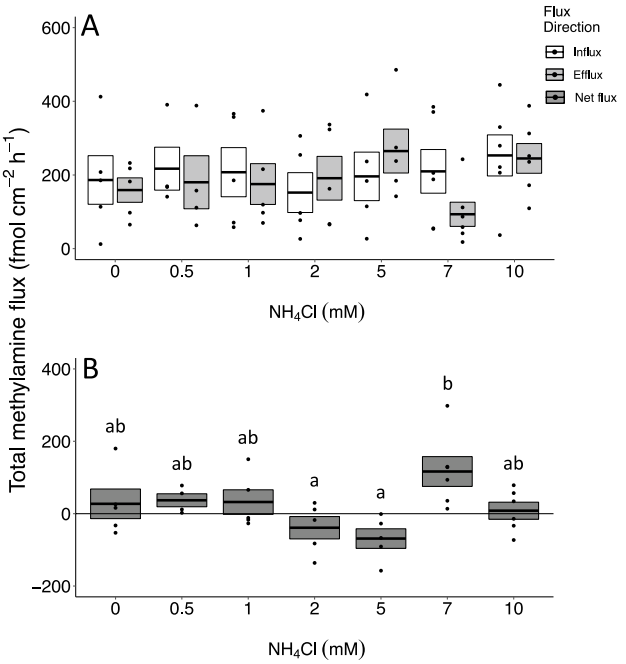

Fig. 4 Total methylamine (MA) flux across intestinal spiral valve folds from 7 day fasted North Pacific spiny dogfish (*Squalus acanthias suckleyi*). Tissues mounted in Ussing chambers and preincubated with NH_4Cl (0–10 mM) for 2 h before preincubation solution was removed, tissues rinsed with fresh Ringer's, and ^{14}C-MA added for 3 h incubation. **A** Influx and efflux; two-way ANOVA, $p<0.05$. **B** Net flux; one-way ANOVA, $p<0.05$. Means not sharing the same letter are significantly different. Horizontal line within the boxplots indicates mean, and the upper and lower box boundaries indicate sem, with individual data points represented as black dots ($n=6$)

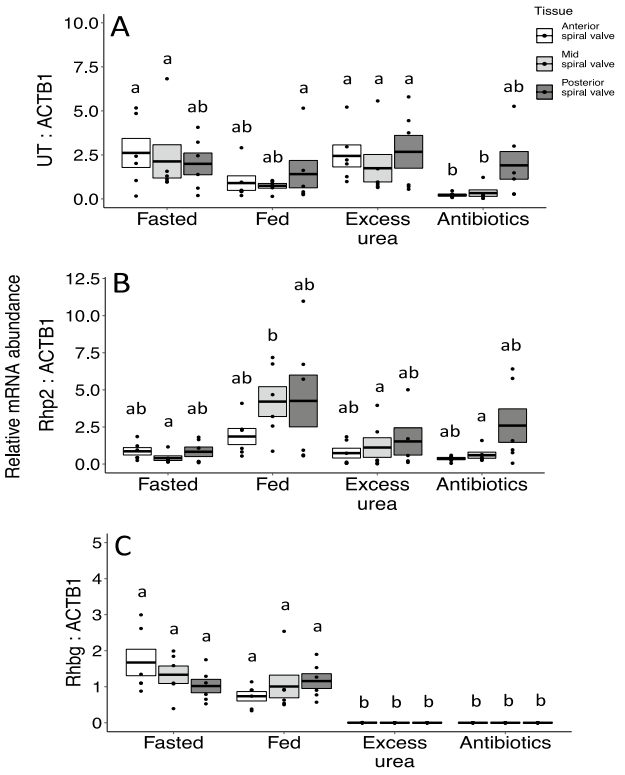

Fig. 5 mRNA abundance of **A** urea transporter (UT), and two ammonia transporters **B** Rhp2 and **C** Rhbg relative to the internal standard ACTB1, in the anterior, mid, and posterior spiral valve of North Pacific spiny dogfish (*Squalus acanthias suckleyi*). Tissues collected from 7 day fasted (Fasted), 20 h post-fed (Fed), 20 h post-fed excess urea (700 mM; Excess urea), and 72 h post-fed and antibiotic administration (Antibiotics). Horizontal line within the boxplots indicates mean, and the upper and lower box boundaries indicate sem, with individual data points represented as black dots ($n=6$). Means not sharing the same letter are significantly different. Two-way ANOVA, $p<0.05$

interaction between concentration and direction ($F_{6,58}=0.6$, $p=0.7$), and no significant differences between influx and efflux at any preincubation concentration ($p>0.1$) (Fig. 4A). For the net flux of total MA, one-way ANOVA showed a significant difference between 7 mM (117 ± 41 *f*mol cm^{-2} h^{-1}) and both 2 mM (-39 ± 31 *f*mol cm^{-2} h^{-1}) and 5 mM (-69 ± 27 *f*mol cm^{-2} h^{-1}) NH_4Cl ($p>0.03$); however, none of the concentrations were significantly different from zero ($p>0.4$). There was no overall net flux of total MA at any NH_4Cl preincubation concentration ($p>0.7$) (Fig. 4B).

mRNA abundance in the spiral valve

To examine the effects of the four treatments (fasted, fed, excess urea, and AB-treated) on the relative mRNA abundance of UT in the six tissues examined (anterior, mid, and posterior spiral valve, gills, kidney, liver), a two-way ANOVA showed a significant interaction between treatment and tissue ($F_{13,110}=4.5$, $p<0.001$). Within the spiral valve, there were no significant differences in UT mRNA abundance between the anterior, mid, and posterior regions for all four treatments ($p>0.9$) (Fig. 5A). Between treatments, the anterior and mid regions of the AB-treated dogfish spiral valve showed significantly lower levels of UT mRNA abundance than that of the fasted and excess urea dogfish ($p<0.02$).

For the mRNA abundance of Rhp2, there was a significant interaction between treatment and tissue ($F_{13,108}=2.8$, $p<0.001$), but no significant differences in Rhp2 mRNA abundance between the intestinal regions ($p>0.4$) (Fig. 5B). Between treatments, the mid spiral valve region of fed dogfish showed significantly higher levels of Rhp2 mRNA than the fasted, excess urea, and AB-treated dogfish ($p<0.05$).

The mRNA abundance of Rhbg has a significant interaction between treatment and tissue ($F_{13,110}=6.1$, $p<0.001$), but no significant difference within treatments for the anterior, mid, and posterior spiral valve regions ($p>0.8$) (Fig. 5C). Between treatments, the fasted and fed dogfish showed significantly higher Rhbg mRNA abundance in all three spiral valve regions than the excess urea and AB-treated dogfish ($p<0.0001$).

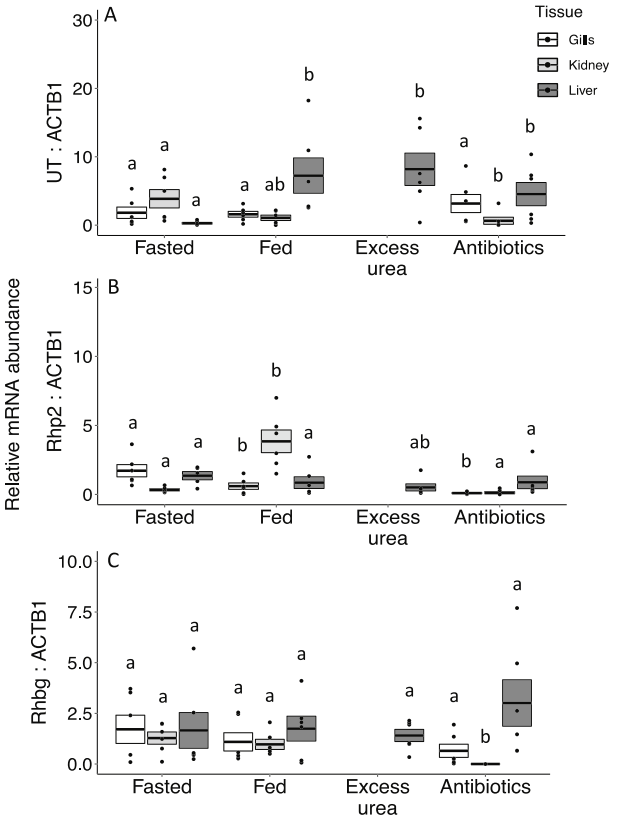

Fig. 6 mRNA abundance of **A** urea transporter (UT), and two ammonia transporters **B** Rhp2 and **C** Rhbg relative to the internal standard ACTB1, in the gills, kidney, and liver of North Pacific spiny dogfish (*Squalus acanthias suckleyi*). Tissues collected from 7 day fasted (Fasted), 20 h post-fed (Fed), 20 h post-fed excess urea (700 mM; Excess urea), and 72 h post-fed and antibiotic administration (Antibiotics). Horizontal line within the boxplots indicates mean, and the upper and lower box boundaries indicate sem, with individual data points represented as black dots ($n = 6$). Means not sharing the same letter are significantly different. Lettering refers to statistical significance within a single tissue across the four treatments; statistical analysis was not conducted between the gills, kidney, and liver. Two-way ANOVA, $p < 0.05$

mRNA abundance in the gills, kidney, and liver

Between treatments, there were no significant differences in UT mRNA abundance in the gills ($p > 0.7$) (Fig. 6A). The kidney of the AB-treated dogfish showed significantly lower levels of UT mRNA abundance than the fasted dogfish ($p < 0.01$), but no difference from the fed dogfish ($p > 0.1$), and no differences in UT mRNA abundance between the fasted and fed animals ($p = 0.2$) (Fig. 6A). The liver of the fasted dogfish showed significantly lower levels of UT mRNA abundance than the other three treatments ($p < 0.01$) (Fig. 6A).

Rhp2 mRNA abundance in the gills showed significantly higher levels in the fasted dogfish compared to the fed and AB-treated dogfish ($p < 0.04$) (Fig. 6B). The kidney of the fed dogfish showed significantly higher levels of Rhp2 mRNA abundance compared to the fasted and AB-treated dogfish ($p < 0.001$). There were no significant differences in Rhp2 mRNA abundance in the liver for any treatment ($p > 0.1$).

For Rhbg mRNA abundance between treatments, there were no significant differences in the gills ($p > 0.5$) or liver ($p > 0.5$) (Fig. 6C). The kidney of the AB-treated dogfish showed significantly lower levels of Rhbg than the fasted and fed dogfish ($p < 0.002$). Statistical analyses were not performed between the gills, kidney, and liver within individual treatments.

Discussion

Bidirectional flux

Our data show that the ability of the spiral valve to move urea and MA does not vary along the length of the intestine from the anterior to posterior region in *S. a. suckleyi*. This was demonstrated by the paired bidirectional Ussing chamber flux studies showing no significant differences in the influx, efflux, and net flux of total urea or total MA across the three spiral valve regions (Figs. 1, 2). The preincubation of the spiral valve folds in NH_4Cl (0–10 mM) was intended to simulate dietary nitrogen in the lumen of a fed animal, and the removal of the NH_4Cl prior to the addition of the radiolabelled substrates was to minimize any potential effects caused by a concentration gradient. This allowed us to examine if lumenal concentrations of ammonia stimulated the expression of the transport proteins, as evidenced by a significant movement of the substrates of interest. For both total urea and total MA, the net movement of the substrates was not affected by any of the NH_4Cl preincubation concentrations (Figs. 3, 4). The in vitro unidirectional uptake of urea across dogfish spiral valve folds was previously shown to be concentration dependent (Anderson et al. 2015), while similar Ussing chamber studies with total MA and total ammonia flux have not been conducted. From our study, it appears the movement of urea and MA were not dependent upon the prestimulation of the transport proteins by nitrogen availability. It is currently unclear why the influx of total urea at 5 and 7 mM NH_4Cl was significantly lower compared to 10 mM, but the resulting net fluxes were not significantly different from one another, or from zero (Fig. 3). Interestingly, there was also a difference in total MA flux between 5 and 7 mM NH_4Cl (as well as 2 mM), but the resulting net fluxes were not significantly different from zero (Fig. 4). Additionally, the influx of total MA across the 0 mM NH_4Cl preincubation concentration was 186 *f*mol cm^{-1} h^{-1}, and the efflux was 159 *f*mol cm^{-1} h^{-1} (Fig. 4A), while the influx across the three spiral valve regions was 101 *f*mol cm^{-1} h^{-1} and the efflux

was 94 *f*mol cm^{-1} h^{-1} (Fig. 2A). The greater flux of total MA in the NH_4Cl experiment (Fig. 4) may be due to the 5 h total experimental period compared to the 3 h period for the regional difference experiment (Fig. 2). The 2 h preincubation period may have led to a buildup of ammonia within the tissue preparation, originating from the catabolism of urea in the Ringer's bathing solution by microbial urease along the epithelium (Wood et al. 2019). Dogfish spiral valve tissue has been shown to be viable for at least 6 h post-sacrifice of the animal (A. M. Weinrauch personal communication). For both experiments, there was no net flux of total MA, regardless of total experimental time.

Our data investigating potential regional differences along the length of the spiral valve (Figs. 1, 2) used 7 day fasted dogfish, and showed no net movement of total urea across the spiral valve tissues. These data differ from previously published reports showing a net efflux of urea across the spiral valve tissues of fasted dogfish (Liew et al. 2013; Anderson et al. 2015). One reason may be that the data we report are not statistically different from zero, indicating no net flux. In the previous studies (Liew et al. 2013; Anderson et al. 2015), values above zero were reported as net influx, and the values below zero were reported as net efflux, but it is unclear if the data were statistically different from zero. Indeed, Liew et al. (2013) reported a net efflux of urea ($-$ 2 µmol cm^{-2} h^{-1}) across in vitro gut sacs of fasted dogfish, and Anderson et al. (2015) reported a net efflux of urea ($\sim -$ 2.5 µmol cm^{-2} h^{-1}) across spiral valve folds mounted in Ussing chambers. In our study, the mean net flux across all three spiral valve regions was 0.83 µmol cm^{-2} h^{-1}, and the high variability of the individual data points account for the net flux not being statistically different from zero. It is unclear how variable the data were from the other studies, but it is possible that the previously reported urea efflux in fasted dogfish may not have been statistically different from zero.

Intestinal transport and mRNA abundance

To examine if access to dietary nitrogen affects the mRNA abundance of the transport proteins, we compared tissues from 7 day fasted and 20 h post-fed via gavage. There were no significant differences in UT mRNA abundance between the fed and fasted dogfish, or across the three spiral valve regions (Fig. 5A). The acquisition of exogenous nitrogen across the spiral valve (Liew et al. 2013) plays a large role in the ability of marine elasmobranchs to maintain whole-body nitrogen homeostasis. In both voluntary and involuntary feeding studies with *S. a. suckleyi*, plasma urea concentrations increased between 20 and 24 h post-feeding (Wood et al. 2005, 2007b, 2010; Kajimura et al. 2006, 2008). Therefore, we had predicted an increase in UT mRNA abundance in the fed dogfish, as a way to increase lumenal urea transport to the plasma necessary to acquire and retain dietary nitrogen, but surprisingly, this was not the case. Indeed, when dogfish were fed excess urea (700 mM), they had similar UT mRNA levels compared to the fed and fasted animals (Fig. 5A). This is surprising as one would assume that these nitrogen-limited animals would want to acquire as much dietary nitrogen as possible to use for osmotic and somatic processes, and an increase in transport protein expression would allow for that. Perhaps, the general lack of a significant difference in the mRNA levels between the groups was due to the method of force-feeding via gavage, as discussed by Hoogenboom et al. (2020). Ingestion of a fish-slurry, rather than whole pieces of prey, may have reduced the need for mechanical breakdown by the GI tract and presumably increased the speed of digestion. Therefore, tissue collection at 20 h post-feeding, intended to match the post-prandial increase in plasma urea concentrations measured in the previous studies (Wood et al. 2005, 2007b, 2010; Kajimura et al. 2006, 2008), may have missed an earlier increase in plasma urea concentrations, and potentially an increase in the transcript abundance of the transport proteins if digestion had progressed at a faster rate.

To examine the role of the GI microbiome on the proposed nitrogen-recycling mechanism (Wood et al. 2019), antibiotics were administered via gavage into the GI tract, and were shown to be effective in virtually eliminating urease activity within the intestinal lumen (MacPherson et al. 2022). The antibiotic treatment significantly reduced UT mRNA abundance in the anterior and mid regions of the AB-treated spiral valve compared to that of the fasted and excess urea dogfish, but not the fed (Fig. 5A). There is currently little research on the effects of antibiotics on nitrogen homeostasis in marine elasmobranchs. Weinrauch et al. (2020) found the in vitro administration of antibiotics to the lumen of intestinal gut sacs from *S. a. suckleyi* induced a non-significant accumulation of ammonia in the lumenal medium, and no difference in the flux of urea across intestinal gut sacs. In the Atlantic stingray, an in vivo application of an antibiotic cocktail (different to the one administered to the dogfish in this study) via oral gavage into the buccal cavity significantly reduced but did not eliminate the GI microbiome, and did not significantly affect plasma urea concentrations (Doucette 2016). The cocktail of antibiotics administered to the AB-treated dogfish all but eliminated microbial urease activity, and induced a reduction in plasma urea at 24 h post-administration (MacPherson et al. 2022). The variable data collected from these three studies highlight the need for more research to elucidate the involvement of the GI microbiome in the catabolism and recycling of nitrogen, and the role it may play on whole-body nitrogen homeostasis for these animals.

The Rhp2 mRNA abundance did not differ across the spiral valve regions or between treatments, except for a significantly higher level in the mid region of the fed dogfish compared to the other three treatments (Fig. 5B). In cloudy catshark (*Scyliorhinus torazame*), Rhp2 was expressed along the brush-border membrane of the intestinal columnar epithelium (Hoogenboom et al. 2023). Due to this apical expression, Rhp2 is likely involved in the uptake of ammonia from the intestinal lumen into the epithelium, and necessary for lumenal ammonia uptake, particularly in fed animals. Similar to the UT, the Rhp2 mRNA levels in the excess urea dogfish were not significantly different from the fed and fasted animals (except for the mid region). Perhaps, as stated above, our sampling time of 20 h missed the post-prandial increase of transporter mRNA abundance due to the assumed decrease in digestion time. Alternatively, as these ureosmotic animals rely on urea, and the cost of acquiring the 700 mM dietary urea would presumably be less energetically expensive than the synthesis of urea (Walsh and Mommsen 2001), perhaps the excess urea fed dogfish focused on the acquisition of urea rather than the acquisition of ammonia.

There were no significant differences in Rhbg mRNA levels across the three spiral valve regions in the fasted and fed dogfish (Fig. 5C). Currently, the localization of Rhbg within the marine elasmobranch intestinal epithelium is unknown; however, Rhbg is generally expressed along the basolateral membrane of epithelial cells (Wright and Wood 2009). If this pattern holds true, Rhbg is likely responsible for moving ammonia from the intestinal cells into the plasma. As ammonia is a toxic molecule, particularly to the central nervous system (Cooper and Plum 1987), the presumptive basolateral localization of Rhbg may mitigate detrimental concentrations of ammonia from entering the plasma. Indeed, there can be a large concentration gradient between the intestinal lumen and plasma, as post-fed lumenal ammonia can exceed 4 mM (Wood et al. 2019; Hoogenboom et al. 2020), while plasma ammonia can range from 0.081 mM (Wood et al. 1995) to 0.25 mM (Wood et al. 2005). Although not investigated in this study, it has been previously shown that urea is synthesized via the OUC within the intestinal epithelial cells, as demonstrated by the presence of OUC enzymes within dogfish spiral valve tissues (Kajimura et al. 2006). We propose that the nitrogen required for the OUC to function is supplied by the ammonia taken up from the intestinal lumen through the apical Rhp2 transport protein. Thus, a concomitant reduction in the presumptive basolateral Rhbg may prevent and/or retard any ammonia, not destined for the OUC, from flooding into the plasma. Indeed, the transcript abundance of Rhp2 in fed dogfish was orders of magnitude higher than Rhbg in the same animals. Additionally, the excess urea dogfish showed very low Rhbg mRNA abundance compared to the fasted and fed dogfish. The 700 mM prandial urea would presumably increase the proliferation of microbial urease activity to capitalize upon the available urea, which in turn would increase lumenal ammonia concentrations, as seen in the excess urea in vitro intestinal sacs that reached 4 mM (Hoogenboom et al. 2020). In response to the microbial production of lumenal ammonia, the lower levels of Rhbg mRNA may limit the entry of ammonia into the plasma. Surprisingly, the AB-treated dogfish also showed significantly lower Rhbg mRNA levels compared to the fasted and fed dogfish. The lumenal ammonia concentrations of the AB-treated dogfish were very low (< 0.05 mM) (MacPherson et al. 2022).

Branchial mRNA abundance

We also examined the effects of dietary nitrogen on UT, Rhp2, and Rhbg mRNA abundance in the gills and kidney (primary sites of nitrogen retention and loss), and liver (primary site of urea synthesis) (Schooler et al. 1966; Goldstein and Forster 1971; Wood et al. 1995; Pärt et al. 1998). The mRNA abundance of the branchial UT was unchanged by the digestive state of the dogfish (Fig. 6A). For branchial Rhp2, fasted dogfish showed significantly higher mRNA abundance levels compared to the fed and AB-treated dogfish (Fig. 6B), but Rhbg did not differ between the three treatments (Fig. 6C). In the AB-treated animals, the ammonia excretion rate was significantly reduced at the time of tissue collection (72 h post-AB administration) (MacPherson et al. 2022). The localization of both branchial Rh proteins in marine elasmobranchs is currently unknown; however, it was proposed that Rhp2 and Rhbg may both be basolaterally located (Nawata et al. 2015a; Wood and Giacomin 2016). If both Rh proteins are on the basolateral membrane of the elasmobranch gill, either one or both may act as a back-transport system to move intracellular ammonia from the gill epithelium back to the plasma (Wood and Giacomin 2016), thus retaining the ammonia from excretion. The similar Rhbg mRNA abundance levels among the three treatments may indicate its role in nitrogen retention, regardless of metabolic state. The higher abundance levels of Rhp2 in the fasted dogfish may either be a mechanism to retain ammonia during times of reduced exogenous (i.e., dietary) nitrogen intake, as part of the proposed back-transporter mechanism moving intracellular nitrogen back to the plasma, or as suggested by Wood and Giacomin (2016), used to acquire environmental ammonia to supplement dietary nitrogen intake. Understanding the location of the ammonia transporters in the gill tissue of the dogfish (basolateral or apical) would help resolve this.

Renal mRNA abundance

The UT mRNA abundance in the kidney was significantly lower in the AB-treated dogfish compared to the fasted but not the fed animals (Fig. 6A). The renal UT is exclusively expressed in the collecting tubules of the banded houndshark, along both the apical and basolateral membranes (Hyodo et al. 2004, 2014; Yamaguchi et al. 2009). It was proposed that the renal UTs, particularly when apically expressed, were responsible for reabsorbing urea from the primary urine to limit renal loss and aid in the regulation of whole-body urea levels (Hyodo et al. 2004; Yamaguchi et al. 2009). In the AB-treated dogfish, there were no differences in plasma urea (~ 400 mM) at the time of sampling (72 h post-feeding) (MacPherson et al. 2022) compared that of a 72 h post-fed or a fasted dogfish (Wood et al. 2007b). Therefore, the reduced UT mRNA abundance in the AB-treated dogfish compared to the fasted dogfish does not appear to be the result of the circulating urea or levels of filtered urea available for reabsorption in the kidneys.

Rhp2 mRNA abundance levels in the kidney were significantly higher in the fed dogfish compared to the fasted and AB-treated (Fig. 6B). Renal Rhp2 was identified on the basolateral membrane of the collecting tubules in the banded houndshark (Nakada et al. 2010). When exposed to increased environmental salinity, renal Rhp2 mRNA abundance increased, indicative of Rhp2 retaining nitrogen from the primary urine for use in the synthesis of urea necessary to osmoregulate in the hyperosmotic environment (Nakada et al. 2010). Our mRNA abundance data show a significant increase in renal Rhp2 in fed dogfish, indicating that it may also work to secrete excess ammonia into the primary urine for excretion, or it may facilitate ammonia excretion during acidosis, as proposed by Nawata et al. (2015b). Alternatively, as Nakada et al. (2010) were unable to resolve the direction of transport in their study, the renal Rhp2 may also work to reabsorb filtered ammonia, once again, in an effort to retain nitrogen necessary for urea synthesis.

For the renal Rhbg, there were significantly lower levels in the AB-treated dogfish than the fed and fasted dogfish (Fig. 6C). Rhbg localization within the elasmobranch kidney is currently unknown; however, in the freshwater white-edged stingray (*Himantura signifier*), renal transcript abundance levels of Rhbg were significantly lower after the rays were transferred from fresh to brackish water (Yeam et al. 2017). The reduced transcript abundance may be indicative of nitrogen conservation for the synthesis of urea necessary to osmoregulate in the brackish water. Indeed, ammonia excretion in the stingrays was significantly reduced following transfer to brackish water (Tam et al. 2003). A reduction in Rhbg levels may act as a regulatory mechanism to reduce the loss of ammonia via renal routes; however, urine flow rates may also decrease with acclimation to increased salinity, which would also affect transport capacity. If the renal Rhbg is responsible for ammonia secretion, the antibiotic interruption of the proposed nitrogen-recycling mechanism in the spiral valve of the AB-treated dogfish may necessitate increased ammonia conservation in the kidney.

Hepatic mRNA abundance

The UT mRNA abundance in the liver was significantly lower in the fasted dogfish compared to the fed, excess urea, and AB-treated dogfish, but there were no significant differences in Rhp2 or Rhbg across the treatments (Fig. 6). As the liver is the primary site of urea synthesis via the OUC (Schooler et al. 1966), it is not surprising that hepatic UT mRNA abundance was significantly higher in the three fed treatments (fed, excess urea, and AB-treated) compared to the fasted, due to an increase in dietary nitrogen available for urea synthesis. It is possible that the hepatic UT trafficks newly synthesized urea from the liver to the plasma for circulation; however, the localization of the elasmobranch hepatic UT is currently unknown.

For all three transport proteins, we report the mRNA abundance levels with the understanding that transcript abundance does not always compare directly to protein expression levels (reviewed by Liu et al. 2016). The conclusions we propose in this study require further exploration, beyond our study, to better understand how nitrogen availability may affect transcript abundance levels differently than protein expression levels, and the subsequent movement of nitrogen across the tissues of marine elasmobranchs.

Conclusion

In this study, we show that there are no differences in total urea or total MA flux across the three spiral valve regions, and the movements of the nitrogenous substrates were not affected by the preincubation of NH_4Cl intended to stimulate the transport proteins. Our data contradict the previous studies that reported a net efflux of urea across the spiral valve tissues of fasted dogfish; we report no net flux. The transcript abundance of the three transport proteins within the intestine was not significantly affected by feeding state, with the exception of an increase in Rhp2 in the mid spiral valve region of fed dogfish, and the application of antibiotics reduced the mRNA levels of UT and Rhbg. The presence of UT, Rhp2, and Rhbg, within the tissues responsible for nitrogen acquisition, retention, and loss speaks to the dynamic system that functions within these animals to coordinate nitrogen trafficking, with the ultimate goal of maintaining whole-body nitrogen homeostasis, regardless of feeding state or metabolic demands.

Acknowledgements We acknowledge the University of Manitoba campuses are located on the original lands of Anishinaabeg, Cree, Oji-Cree, Dakota, and Dene peoples, and on the homeland of the Métis Nation. We acknowledge that Bamfield Marine Sciences Centre sits on the Huu-ay-aht and Maa-nulth Treaty lands, and is the traditional territory of the Huu-ay-aht First Nation. We thank Jessica Macpherson, Alexandra Schoen, Dr. Alyssa Weinrauch, and Dr. Carol Bucking for their gracious help with sample collection, as well as Dr. Alex Quijada Rodriguez and Ashley Tripp for help with sample analysis. We thank the Research Coordinator Dr. Eric Clelland, and Head of Research Services Tao Eastham for invaluable help while conducting research at BMSC.

Author contributions All authors have contributed to the study conception and design. Material preparation, data collection, and analyses were performed by JLH. The first draft of the manuscript was written by JLH and all authors commented on previous versions of the manuscript. All authors read and approved the final manuscript.

Funding Research was supported by Natural Sciences and Engineering Research Council of Canada (NSERC) Discovery Grant to W.G.A. (05348) and the Faculty of Science Fieldwork Support Program from the University of Manitoba. J.L.H. was supported by NSERC Alexander Graham Bell Canada Graduate Scholarship–D.

Data availability The data that support the findings of this study are available from the corresponding author, JLH, upon reasonable request.

Declarations

Conflict of interest The authors declare that they have no known competing financial interests or personal relationships that could have appeared to influence the work reported in this paper.

References

Anand U, Anand CV (1993) The energy cost of urea synthesis. Biomed Educ 21:198–199. https://doi.org/10.1016/0307-4412(93)90095-H

Anderson PM (1991) Glutamine-dependent urea synthesis in elasmobranch fishes. Biochem Cell Biol 69:317–319. https://doi.org/10.1139/o91-049

Anderson PM, Casey CA (1984) Glutamine-dependent synthesis of citrulline by isolated hepatic mitochondria from *Squalus acanthias*. J Biol Chem 259:456–462. https://doi.org/10.1016/S0021-9258(17)43682-9

Anderson WG, Dasiewicz PJ, Liban S et al (2010) Gastro-intestinal handling of water and solutes in three species of elasmobranch fish, the white-spotted bamboo shark, *Chiloscyllium plagiosum*, little skate, *Leucoraja erinacea* and the clear nose skate *Raja eglanteria*. Comp Biochem Physiol A 155:493–502. https://doi.org/10.1016/j.cbpa.2009.09.020

Anderson WG, McCabe C, Brandt C, Wood CM (2015) Examining urea flux across the intestine of the spiny dogfish, *Squalus acanthias*. Comp Biochem Physiol A 181:71–78. https://doi.org/10.1016/j.cbpa.2014.11.023

Bucking C (2015) Feeding and digestion in elasmobranchs: tying diet and physiology together. In: Shadwick RE, Farrell AP, Brauner CJ (eds) Fish physiology. Academic Press, New York, pp 347–394

Chatchavalvanich K, Marcos R, Poonpirom J et al (2006) Histology of the digestive tract of the freshwater stingray Himantura signifer Compagno and Roberts, 1982 (Elasmobranchii, Dasyatidae). Anat Embryol (berl) 211:507–518. https://doi.org/10.1007/s00429-006-0103-3

Cooper AJL, Plum F (1987) Biochemistry and physiology of brain ammonia. Physiol Rev 67:440–519. https://doi.org/10.1152/physrev.1987.67.2.440

Doucette KK (2016) The elasmobranch-microbe relationship: trimethylamine N-oxide synthesis, urea hydrolysis, and microbe-osmolyte interactions in the Atlantic stingray, *Dasyatis sabina*. The University of Sounthern Mississippi

Goldstein L, Forster RP (1971) Urea biosynthesis and excretion in freshwater and marine elasmobranchs. Comp Biochem Physiol 39B:415–421. https://doi.org/10.1016/0305-0491(71)90186-6

Hoogenboom JL, Weinrauch AM, Wood CM, Anderson WG (2020) The effects of digesting a urea-rich meal on North Pacific spiny dogfish (*Squalus acanthias suckleyi*). Comp Biochem Physiol A 249:110775. https://doi.org/10.1016/j.cbpa.2020.110775

Hoogenboom JL, Wong MK-S, Hyodo S, Anderson WG (2023) Nitrogen transporters along the intestinal spiral valve of cloudy catshark (*Scyliorhinus torazame*): Rhp2, Rhbg, UT. Comp Biochem Physiol A Mol Integr 280:111418. https://doi.org/10.1016/j.cbpa.2023.111418

Hyodo S, Kakumura K, Takagi W et al (2014) Morphological and functional characteristics of the kidney of cartilaginous fishes: with special reference to urea reabsorption. Am J Physiol Regul Integr Comp Physiol 307:R1381–R1395. https://doi.org/10.1152/ajpregu.00033.2014

Hyodo S, Katoh F, Kaneko T, Takei Y (2004) A facilitative urea transporter is localized in the renal collecting tubule of the dogfish *Triakis scyllia*. J Exp Biol 207:347–356. https://doi.org/10.1242/jeb.00773

Janech MG, Fitzgibbon WR, Chen R et al (2003) Molecular and functional characterization of a urea transporter from the kidney of the Atlantic stingray. Am J Physiol Ren Physiol 284:F996–F1005. https://doi.org/10.1152/ajprenal.00174.2002

Janech MG, Fitzgibbon WR, Nowak MW et al (2006) Cloning and functional characterization of a second urea transporter from the kidney of the Atlantic stingray, *Dasyatis sabina*. Am J Physiol Regul Integr Comp Physiol 291:844–853. https://doi.org/10.1152/ajpregu.00739.2005

Janech MG, Gefroh HA, Cwengros EE et al (2008) Cloning of urea transporters from the kidneys of two batoid elasmobranchs: evidence for a common elasmobranch urea transporter isoform. Mar Biol 153:1173–1179. https://doi.org/10.1007/s00227-007-0889-4

Jones BC, Geen GH (1977) Food and feeding of spiny dogfish (*Squalus acanthias*) in British Columbia waters. J Fish Res Board Can 34:2056–2066

Kajimura M, Walsh PJ, Mommsen TP, Wood CM (2006) The dogfish shark (*Squalus acanthias*) increases both hepatic and extrahepatic ornithine urea cycle enzyme activities for nitrogen conservation after feeding. Physiol Biochem Zool 79:602–613

Kajimura M, Walsh PJ, Wood CM (2008) The spiny dogfish *Squalus acanthias* L. maintains osmolyte balance during long-term starvation. J Fish Biol 72:656–670. https://doi.org/10.1111/j.1095-8649.2007.01756.x

Leigh SC, Summers AP, Hoffmann SL, German DP (2021) Shark spiral intestines may operate as Tesla valves. Proc R Soc B Biol Sci. https://doi.org/10.1098/rspb.2021.1359

LeMoine CMR, Walsh PJ (2015) Evolution of urea transporters in vertebrates: adaptation to urea's multiple roles and metabolic sources. J Exp Biol 218:1936–1945. https://doi.org/10.1242/jeb.114223

Liew HJ, De Boeck G, Wood CM (2013) An in vitro study of urea, water, ion and CO_2/HCO_3-transport in the gastrointestinal tract of the dogfish shark (*Squalus acanthias*): the influence of feeding. J Exp Biol 216:2063–2072. https://doi.org/10.1242/jeb.082313

Liu Y, Beyer A, Aebersold R (2016) On the dependency of cellular protein levels on mRNA abundance. Cell 165:535–550. https://doi.org/10.1016/j.cell.2016.03.014

MacPherson J, Weinrauch AM, Anderson WG, Bucking C (2022) The gut microbiome may influence post-prandial nitrogen handling in an elasmobranch, the Pacific spiny dogfish (*Squalus suckleyi*). Comp Biochem Physiol A 272:111269. https://doi.org/10.1016/j.cbpa.2022.111269

Marini A-M, Matassi G, Raynal V et al (2000) The human Rhesus-associated RhAG protein and a kidney homologue promote ammonium transport in yeast. Nat Genet 26:341–344. https://doi.org/10.1038/81656

Marini A-M, Urrestarazu A, Beauwens R, André B (1997) The Rh (rhesus) blood group polypeptides are related to NH_4^+ transporters. Trends Biochem Sci 22:460–461. https://doi.org/10.1016/S0968-0004(97)01132-8

Mobley HLT, Hausinger RP (1989) Microbial ureases: significance, regulation, and molecular characterization. Microbiol Rev 53:85–108. https://doi.org/10.1128/mmbr.53.1.85-108.1989

Morgan RL, Ballantyne JS, Wright PA (2003) Regulation of a renal urea transporter with reduced salinity in a marine elasmobranch, *Raja erinacea*. J Exp Biol 206:3285–3292. https://doi.org/10.1242/jeb.00554

Nakada T, Westhoff CM, Yamaguchi Y et al (2010) Rhesus glycoprotein P2 (Rhp2) is a novel member of the Rh family of ammonia transporters highly expressed in shark kidney. J Biol Chem 285:2653–2664. https://doi.org/10.1074/jbc.M109.052068

Nawata CM, Walsh PJ, Wood CM (2015a) Physiological and molecular responses of the spiny dogfish shark (*Squalus acanthias*) to high environmental ammonia: scavenging for nitrogen. J Exp Biol 218:238–248. https://doi.org/10.1242/jeb.114967

Nawata CM, Walsh PJ, Wood CM (2015b) Nitrogen metabolism, acid–base regulation, and molecular responses to ammonia and acid infusions in the spiny dogfish shark (*Squalus acanthias*). J Comp Physiol B 185:511–525. https://doi.org/10.1007/s00360-015-0898-4

Pärt P, Wright PA, Wood CM (1998) Urea and water permeability in dogfish (*Squalus acanthias*) gills. Comp Biochem Physiol A 119:117–123. https://doi.org/10.1016/S1095-6433(97)00400-5

Rao X, Huang X, Zhou Z, Lin X (2013) An improvement of the 2^(-delta delta CT) method for quantitative real-time polymerase chain reaction data analysis. Biostat Bioinform Biomath 3:71–85

R Core Team (2017) R: a language and environment for statistical computing. R Foundation for Statistical Computing, Vienna, Austria

Schooler JM, Goldstein L, Hartman SC, Forster RP (1966) Pathways of urea synthesis in the elasmobranch, Squalus acanthias. Comp Biochem Physiol 18:271–281

Smith CP, Wright PA (1999) Molecular characterization of an elasmobranch urea transporter. Am Physiol Soc Regul Integr Comp Physiol 276:R622–R626. https://doi.org/10.1016/S0016-5085(77)80340-5

Smith HW (1929) The composition of the body fluids of elasmobranchs. J Biol Chem 81:407–419

Smith HW (1936) The retention and physiological role of urea in the elasmobranchii. Biol Rev 11:49–82. https://doi.org/10.1111/j.1469-185X.1936.tb00497.x

Stewart GS, Smith CP (2005) Urea nitrogen salvage mechanisms and their relevance to ruminants, non-ruminants and man. Nutr Res Rev 18:49–62. https://doi.org/10.1079/nrr200498

Tam WL, Wong WP, Loong AM et al (2003) The osmotic response of the Asian freshwater stingray (Himantura signifer) to increased salinity: a comparison with marine (*Taeniura lymma*) and Amazonian freshwater (*Potamotrygon motoro*) stingrays. J Exp Biol 206:2931–2940. https://doi.org/10.1242/jeb.00510

Walsh PJ, Mommsen TP (2001) Evolutionary considerations of nitrogen metabolism and excretion. In: Nitrogen excretion, fish physiology, pp 1–30

Weinrauch AM, Folkerts EJ, Blewett TA et al (2020) Impacts of low salinity exposure and antibiotic application on gut transport activity in the Pacific spiny dogfish, *Squalus acanthias suckleyi*. J Comp Physiol B 190:535–545. https://doi.org/10.1007/s00360-020-01291-4

Westhoff CM, Ferreri-Jacobia M, Mak D-OD, Foskett JK (2002) Identification of the erythrocyte Rh blood group glycoprotein as a mammalian ammonium transporter. J Biol Chem 277:12499–12502. https://doi.org/10.1074/jbc.C200060200

Wickham H (2009) ggplot2: elegant graphics for data analysis

Wood CM (2001) Influence of feeding, exercise, and temperature on nitrogen metabolism and excretion. In: Wright PA, Anderson PM (eds) Fish physiology: nitrogen excretion, 20th edn. Academic Press, New York, pp 201–238

Wood CM, Bucking C, Fitzpatrick J, Nadella SR (2007a) The alkaline tide goes out and the nitrogen stays in after feeding in the dogfish shark, *Squalus acanthias*. Respir Physiol Neurobiol 159:163–170. https://doi.org/10.1016/j.resp.2007.06.008

Wood CM, Giacomin M (2016) Feeding through your gills and turning a toxicant into a resource: how the dogfish shark scavenges ammonia from its environment. J Exp Biol 219:3218–3226. https://doi.org/10.1242/jeb.145268

Wood CM, Kajimura M, Bucking C, Walsh PJ (2007b) Osmoregulation, ionoregulation and acid-base regulation by the gastrointestinal tract after feeding in the elasmobranch (*Squalus acanthias*). J Exp Biol 210:1335–1349. https://doi.org/10.1242/jeb.02736

Wood CM, Kajimura M, Mommsen TP, Walsh PJ (2005) Alkaline tide and nitrogen conservation after feeding in an elasmobranch (*Squalus acanthias*). J Exp Biol 208:2693–2705. https://doi.org/10.1242/jeb.01678

Wood CM, Liew HJ, De Boeck G et al (2019) Nitrogen handling in the elasmobranch gut: a role for microbial urease. J Exp Biol 222:jeb194787. https://doi.org/10.1242/jeb.194787

Wood CM, Pärt P, Wright PA (1995) Ammonia and urea metabolism in relation to gill function and acid-base balance in a marine elasmobranch, the spiny dogfish (*Squalus acanthias*). J Exp Biol 198:1545–1558

Wood CM, Walsh PJ, Kajimura M et al (2010) The influence of feeding and fasting on plasma metabolites in the dogfish shark (*Squalus acanthias*). Comp Biochem Physiol A 155:435–444. https://doi.org/10.1016/j.cbpa.2009.09.006

Wright PA, Wood CM (2009) A new paradigm for ammonia excretion in aquatic animals: role of Rhesus (Rh) glycoproteins. J Exp Biol 212:2303–2312. https://doi.org/10.1242/jeb.023085

Yamaguchi Y, Takaki S, Hyodo S (2009) Subcellular distribution of urea transporter in the collecting tubule of shark kidney is dependent on environmental salinity. J Exp Zool Part A 311:705–718. https://doi.org/10.1002/jez.558

Yeam CT, Chng YR, Ong JLY et al (2017) Molecular characterization of two Rhesus glycoproteins from the euryhaline freshwater white-rimmed stingray, *Himantura signifer*, and changes in their transcript levels and protein abundance in the gills, kidney, and liver during brackish water acclimation. J Comp Physiol B 187:911–929. https://doi.org/10.1007/s00360-017-1067-8

Zar JH (1984) Biostatistical analysis, 2nd edn. Prentice-Hall, Eaglewood Cliffs